# **Network Formation and Dynamics Among Multi-LLMs**

MARIOS PAPACHRISTOU, Cornell University, USA YUAN YUAN, Purdue University, USA

Social networks influence behaviors, preferences, and relationships and play a crucial role in the dissemination of information and norms within human societies. As large language models (LLMs) increasingly integrate into social and professional environments, understanding their behavior within the context of social networks and interactions becomes essential. Our study analyzes the behaviors of standard network structures and real-world networks to determine whether the dynamics of multiple LLMs align with human social dynamics. We explore various social network principles, including micro-level concepts such as preferential attachment, triadic closure, and homophily, as well as macro-level concepts like community structure and the small-world phenomenon. Our findings suggest that LLMs demonstrate all these principles when they are provided with network structures and asked about their preferences regarding network formation. Furthermore, we investigate LLMs' decision-making based on real-world networks to compare the strengths of these principles. Our results reveal that triadic closure and homophily have a stronger influence than preferential attachment and that LLMs substantially exceed random guessing in the task of network formation predictions. Overall, our study contributes to the development of socially aware LLMs by shedding light on LLMs' network formation behaviors and exploring their impacts on social dynamics and norms.

Additional Key Words and Phrases: large language models, networks, network formation, link prediction, multi-agent systems

#### 1 INTRODUCTION

Recent progress in large language models (LLMs), such as GPT [50] and LLaMA2 [58], have underscored the importance of understanding AI behavior. It is crucial to comprehend AI actions to ensure they align with human expectations, mitigate potential risks, and maximize their benefits. Misaligned AI actions can lead to unintended consequences, such as biased decision-making, fairness issues, and the miscoordinative or non-cooperative behavior [56]. Additionally, researchers have started to apply specific social science methodologies to study LLMs, including methods analogous to laboratory experiments, agent-based modeling, and qualitative methods. These methods help uncover the generative capabilities of LLMs and their interpretability from a rigorous social science perspective [15, 29, 36, 53].

In human societies, social networks play a crucial role in shaping individual behaviors, preferences, and connections, as well as influencing the diffusion of information and norms across communities [4, 5, 23, 57]. LLMs have shown great potential in social contexts, notably as intelligent personal assistants facilitating social and business interactions (see, e.g., [16, 52, 61]). However, less is known about how LLMs' innate behaviors and preferences align with human network formation principles [30, 53, 64].

Our study explores LLMs' behaviors and preferences in network formation in both synthetic and real-world networks. By analyzing interactions among multiple LLMs (or multi-LLMs), we aim to understand the implications of LLMs representing humans in social and business settings. Specifically, we examine micro-level social network properties including preferential attachment [7], triadic closure [25], and homophily [44], as well as macro-level properties including community structure [49], and the small-world phenomenon [34, 63].

In synthetic networks, our findings reveal that LLMs can generate networks exhibiting preferential attachment and following scale-free degree distributions. Moreover, LLMs demonstrate strong tendencies toward triadic closure and exhibit significant homophily. These behaviors explain the emergence of community structures with high modularity in networks formed by multiple LLMs.

### **ALGORITHM 1:** Prompt used to implement $Q(A_t, i_t, \delta)$ formatted as a Python f-string.

Additionally, we show that LLM agents exhibit dynamics consistent with small-world phenomena akin to those observed in the Watts-Strogatz model [63].

Next, we compare across these principles and uncover the main drivers of network dynamics among these factors. To do this, we consider real-world networks and ask each LLM to simulate a node in the network. We provide information on their network structure and ask for their decisions for the next link formation or dissolution step. We approach this problem as a discrete choice modeling problem [41, 51]. In this real-world setting, we find that LLMs' choices are primarily weighted on homophily and triadic closure, compared to preferential attachment, and that LLMs substantially exceed random guessing when predicting new links. Additionally, the resulting choices of LLM agents strengthen the network's community structure.

Our study contributes to the literature on large language models (LLMs) in several ways. First, it advances the discussion on aligning LLMs with human social preferences, which has potential applications in developing socially aware LLMs for real-life interactions. Understanding the behaviors of LLMs in social network formation can inform the alignment of these models with human social preferences. Additionally, this study serves as a step toward developing LLMs that are more socially aware and sensitive to human preferences, enhancing their effectiveness and acceptability in social contexts. Insights into LLMs' innate behaviors in network formation can inform the design of LLMs for effective collaboration in social and professional settings. Finally, our study could contribute to understanding the impact of LLMs on social dynamics and norms, including their role in facilitating or hindering social change and the adoption of new behaviors.

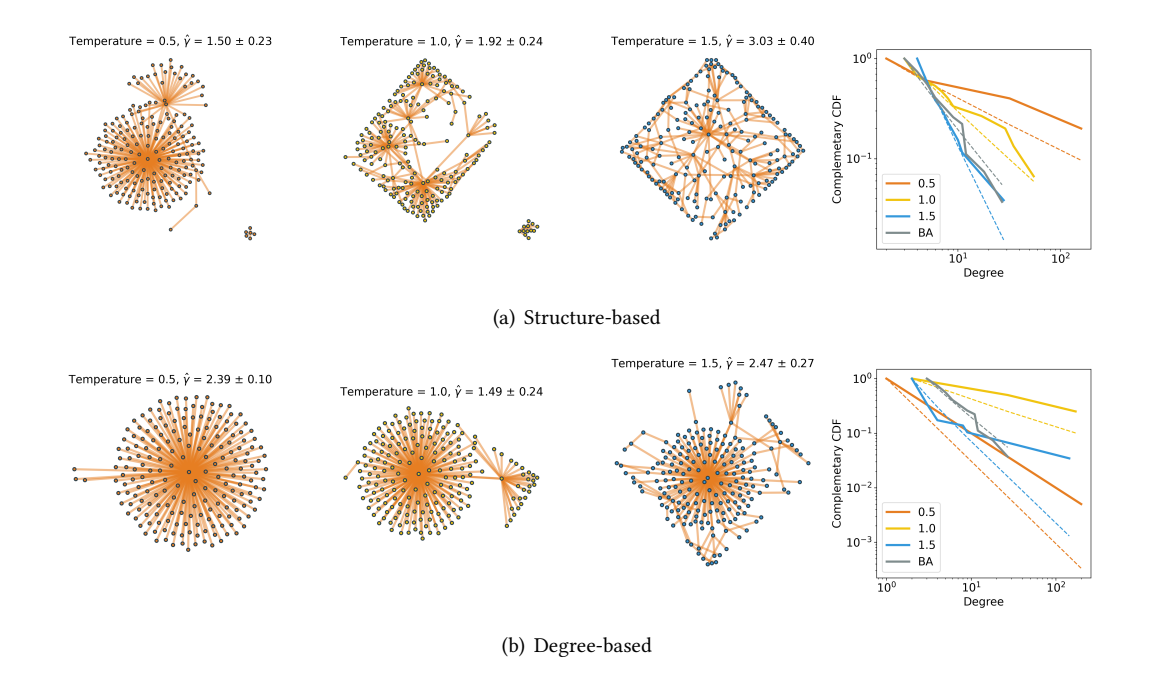


Fig. 1. Networks with n=200 nodes created based on Principle 1 for various temperatures. For the structure-based networks (Figure 1(a)), we provide the multi-LLMs with the neighborhoods  $\{N_{j,t}: j \in i_t\}$ , and for the degree-based networks (Figure 1(b)), we provide the degrees  $\{d_{j,t}: j \in i_t\}$  of the nodes  $j \in i_t$ . We also plot the degree distribution and compare it against a BA network with n=200 nodes. **Top:** In Figure 1(a), we observe that the resulting networks follow a power-law degree distribution (P>0.5, Bootstrap hypothesis test). When the temperature is 1.5, the resulting network resembles the BA model (P<0.001, K-S test). **Bottom:** When the degree information is provided only (Figure 1(b)), the resulting networks correspond to unrealistic star-like formations that are far from a scale-free network and resemble more a core-periphery network.

#### 2 METHODS

Our study employs the state-of-the-art LLMs, such as GPT-3.5 and GPT-4 [50] with the OpenAI API<sup>1</sup>. We constructed multiple LLMs using multiple independent conservation threads where each thread represents one multi-LLM. We prompt each LLM by providing information about other LLMs' network information as well as decisions they are faced with. We test both state-of-the-art GPT-based models: for the results of Sections 3.1 and 3.2, we use GPT-3.5 agents, and in Section 3.3, we use GPT-4 agents. We obtained similar results using GPT-3.5 and GPT-4. Overall, we adopted a standard framework for multi-LLMs but underscored the multi-agent nature of the design in our setting [2, 3, 14, 20, 36].

#### 2.1 Procedure

In our study, we performed experiments to assess whether key network principles at both the micro-level (such as preferential attachment, triadic closure, and homophily) and the macro-level

<sup>&</sup>lt;sup>1</sup>For GPT-3.5 we use the gpt-3.5-turbo model provided by OpenAI, and for GPT-4 we use the gpt-4-1106-preview model.

(including community structure and weak ties) align with classical network models. Subsequently, we utilized real-world networks to determine the factors that are most heavily weighted by LLMs.

Our experiments span a time series of T steps, with a sequence of network structures denoted as  $G_1, G_2, \ldots, G_T$ . The initial network,  $G_1$ , is referred to as the *seed network*. At each step t, we select a *query node*  $i_t$  (which may either be a new arrival or an existing node in the graph) and assign it the task of forming new links. This is accomplished by selecting nodes from a set of alternatives  $A_t$  (meaning potential candidates for link formation) and initiating a query call  $Q(A_t, i_t, \delta)$  to the LLM (as outlined in Algorithm 1) to create up to  $\delta$  new links. The edge set selection process involves presenting the LLMs with personal or network features of the alternatives, denoted as  $F(A_t) = \{f_a : a \in A_t\}$ , which may include information such as the neighbors of the nodes, node degrees, common connections with  $i_t$ , and community memberships, formatted in JSON. We adopt a zero-shot learning approach, avoiding the provision of examples to the model to prevent bias, in line with relevant studies such as [14]. This approach allows for the exploration of the innate preferences of LLMs.

We employ multiple temperatures to account for the variability in response generation by LLM systems, which is also observed in classical statistical models of network formation [30]. Our study conducts experiments using three temperatures: 0.5, 1.0, and 1.5.

Moreover, the model is tasked with outputting a JSON object indicating the node chosen for link formation and the rationale behind the choice.

#### 3 RESULTS

In this section, we discuss three major micro-level network principles: preferential attachment, triadic closure, and homophily. We then examine two macro-level network principles: community structure and small-world phenomenon. Subsequently, we test the strength of these principles when LLM agents face real-world networks and compare the preferences in network formation tasks between LLMs and humans.

#### 3.1 Micro-Level Properties

*Principle 1: Preferential Attachment.* Preferential attachment is a well-known mechanism in network science that explains how certain nodes in a network become more connected over time, leading to the emergence of highly connected vertices and scale-free distribution of degree [7, 8].

We examine whether LLMs exhibit the preferential attachment mechanism in the following way: First, we start with an empty network and add nodes at each time step t. For each new time step, we add a new node  $i_t$ , providing information on the network neighbors of all existing nodes<sup>2</sup>. We generated networks with n = 200 nodes.

We plot one of the examples of resulting networks under each temperature in Figure 1(a). As observed in all temperature setups, we observe a few nodes that have many connections, and the majority of the notes have one or few connections, which renders the degree distribution scale-free, i.e., the probability  $\pi(d)$  a node has degree d is given by

$$\pi(d) \propto d^{-\gamma}$$
, where  $\gamma > 1$ .

Furthermore, we observe mode "super nodes" with many connections as the temperature increases. We also compare with the Barabási–Albert (BA) model [7] where each incoming node t, the probability  $p_{i,t}$  of it connecting to node i is proportional to  $d_{i,t}$ , where  $d_{i,t}$  is the degree of node i at

<sup>&</sup>lt;sup>2</sup>See Appendix B, for information about how the features are represented in the prompt.

#### Reasoning for Principle 1

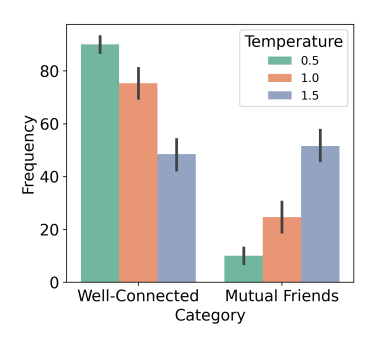


Fig. 2. Distribution of reasoning across categories for the networks of Figure 1(a). The classification is done using GPT-3.5 on a set of 20 randomly sampled reasons repeated over five times (frequencies are microaveraged). The error bars correspond to 95% confidence intervals.

time step t, namely,

$$p_{i,t} = \frac{d_{i,t}}{\sum_{j=1}^{t} d_{j,t}}.$$

We find that for temperatures being 0.5 and 1.0, although  $\hat{\gamma}=1.50\pm0.23$  and 1.92  $\pm$  0.24, respectively, the degree distribution does not resemble the degree distribution of the generated BA network, where the *P*-values satisfy P<0.001 and P<0.05 respectively (two-sample K-S test compared to the empirical degree distribution of the BA network<sup>3</sup>). However, when the temperature is 1.5, the LLM-generated networks resemble the BA model, where we have P>0.9 (two-sample K-S test compared to the empirical degree distribution of the BA network) and have  $\hat{\gamma}=3.03\pm0.40$ .

Moreover, for all temperatures, the resulting degree distribution is scale-free (P > 0.5, bootstrapping hypothesis test comparing with the fitted scale-free distribution).

We also examine the network formation when only degree information (rather than network structure) is provided, in a similar spirit of [20]. We present the results in Figure 1(b). We observe "star-like" formations around one node. The degree distributions differ from scale-free distributions produced by statistical models such as the BA model (P < 0.001, two-sample K-S test compared to the empirical distribution of the generated BA network), and are closer to a core-periphery network [13].

Finally, we employ text analysis of reasoning provided by the agents for the results of Figure  $1(a)^4$ . We observe two main categories of reasons (see Figure 2 for the fraction under each temperature):

- Well-Connectedness: it corresponds to reasons related to the person being well-connected and having many friends.
- *Mutual Friends*: it is related to having many friends in common with the person so that the person can introduce them to their friends.

The well-connectedness reason becomes less prevalent as the temperature increases, and the mutual friends' reason becomes more prevalent. Note that when the temperature is 1.5, the two reasons have almost the same frequency.

<sup>&</sup>lt;sup>3</sup>As [6] showed, the BA model follows the scale-free distribution of the form  $\pi_{\rm BA}(d) \propto d^{-3}$  for sufficiently large n. However, because here n is small, we instead compared directly to the sample from the BA model which has  $\hat{\gamma}_{\rm BA} = 2.24 \pm 0.24$  instead of comparing with the limiting distribution  $\pi_{\rm BA}(d)$ .

<sup>&</sup>lt;sup>4</sup>We do not provide the distribution of reasons for the results of Figure 1(b) as all of the LLM's decisions are made given the degree information.

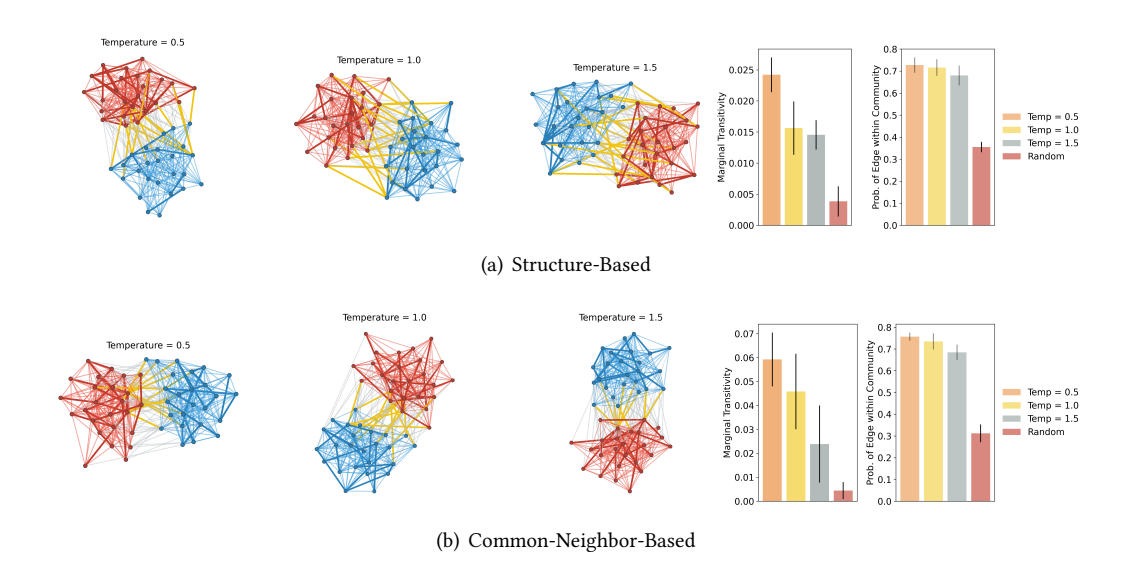


Fig. 3. Networks created based on Principle 2. **Top:** Figure 3(a) shows the resulting networks created by Principle 2 when the intersection of the neighborhoods of the query node and each alternative is provided. The node colors correspond to the stochastic block model (SBM) groups each node belongs to. The red edges correspond to the newly created edges between nodes of the red cluster, the blue edges correspond to the newly created edges between nodes of the blue cluster, and the orange edges correspond to edges created between the two clusters. The newly formed edges are drawn with a larger line width. We observe that the probability of forming an edge within the same community and the marginal transitivity, which indicate triadic closure, is significantly larger than randomly creating links (P < 0.001, t-test). **Bottom:** Figure 3(b) shows the same networks with the only change that instead of the intersection of neighborhoods between the query node and each alternative, we provide the number of common neighbors (i.e., the size of the intersection) between the query node and each alternative. Similarly, we observe that the probability of forming an edge within the same community and the marginal transitivity, which indicate triadic closure, is significantly larger than randomly creating links (P < 0.001, t-test).

Taken together, networks created by LLM systems, when given a network structure, demonstrate preferential attachment and exhibit scale-free degree distributions.

*Principle 2: Triadic Closure.* The second micro-level principle we examine is triadic closure, which describes the phenomenon that individuals are likely to form connections with their friends' friends, leading to closed triangles within the network. This tendency enhances the network's structure and cohesion, rooted in the likelihood of two nodes forming a direct connection if they share a common neighbor [25, 46].

To test for triadic closure, we use an assortative stochastic block model (SBM) [47] to generate an initial seed network  $G_1$  with n nodes divided into two equal-sized clusters A and B. Connections within each cluster have a probability of 0.5, while connections across clusters have a probability of 0.1. This setup reflects our intuition that nodes within the same cluster are more likely to form connections due to their higher number of common neighbors. We then iterate over each node i, providing features based on the intersection of the neighborhoods of all of i's non-neighbors or the number of common friends between i and any non-neighbor j. This modeling choice contrasts the results mentioned about preferential attachment, where the neighborhood information is provided and made to make the two settings consistent.

#### Reasoning for Principle 2

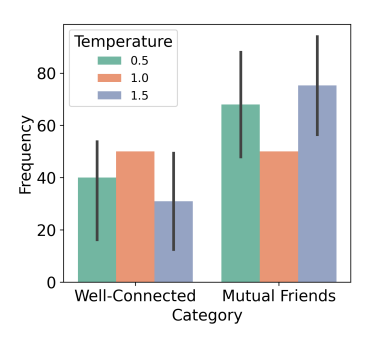


Fig. 4. Distribution of reasoning across categories for the networks of Figure 3(a). The classification is done using GPT-3.5 on a set of 20 randomly sampled reasons repeated over 5 times (frequencies are micro-averaged). The error bars correspond to 95% confidence intervals.

We compare this with the random null model, which selects a node at random to connect to. We run ten simulations for n = 50 nodes.<sup>5</sup>

To measure whether the principle of triadic closure exists, we measure the *fraction*  $\hat{p}$  of newly added edges between nodes of the same community, i.e., the fraction of edges in  $G_T \setminus G_1$  that have their ends both at either A or B, namely

$$\hat{p} = \frac{\left|\left\{\left\{i, j\right\} \in E(G_T) \setminus E(G_1) : y_i = y_j\right\}\right|}{\left|E(G_T) \setminus E(G_1)\right|},$$

where  $y_i, y_j \in \{A, B\}$  are the community memberships of nodes i and j respectively, and  $E(G_T) \setminus E(G_1)$  corresponds to the newly added edges.

Generally, a value of  $\hat{p} > 0.5$  indicates the tendency of triadic closure since an LLM agent, which is supposed to exhibit triadic closure given the common neighbors, would ideally create a link within the same cluster.

Additionally, we report the *marginal transitivity* D of the network, which is defined as the change in the fraction of triangles in the network to open triads from  $G_T$  to  $G_1$  (which corresponds to the SBM), i.e.

$$D = 3 \times \frac{\# \operatorname{triangles}(G_T)}{\# \operatorname{triads}(G_T)} - 3 \times \frac{\# \operatorname{triangles}(G_1)}{\# \operatorname{triads}(G_1)}.$$

We present our simulation results in Figure 3(a). We depict the sample outcomes in Figure 3(a), where the upper panel presents the results when the entire network structure is provided, whereas the lower panel only provides the number of common neighbors. Node colors correspond to their respective groups within the SBM. Red edges denote connections within the red cluster, blue edges within the blue cluster, and orange edges between the two clusters. Newly established edges are emphasized with a thicker line width.

We present the probabilities of network formation within a community in the last panels in each row. We find that the probability of forming a within-community tie across all temperatures is substantially larger than the random network formation scenario (P < 0.001, t-test comparing to

<sup>&</sup>lt;sup>5</sup>For better visualization, we chose n = 50 nodes instead of a large number of nodes such as n = 200. Moreover, the results are statistically significant even with n = 50 nodes.

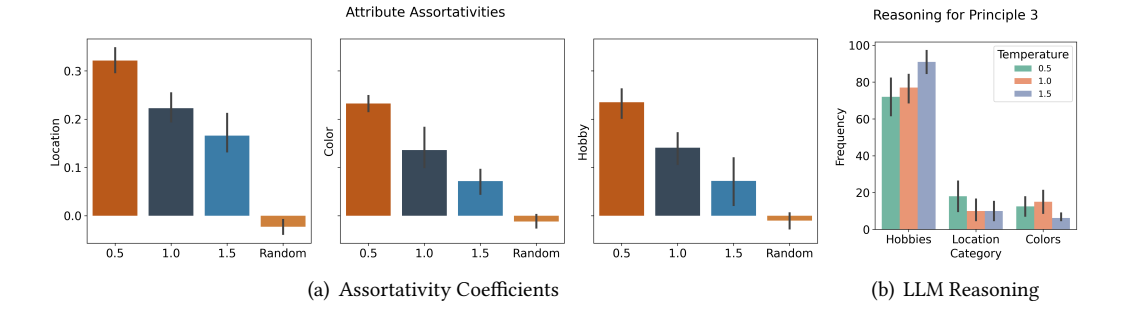


Fig. 5. **Left:** Figure 5(a) shows the assortativity coefficients for each network attribute created based on Principle 3. Each node can form at most  $\delta=5$  links with the other nodes based on their attributes. We observe that for all temperatures, we have positive assortativity (P<0.001, t-test with 0), which indicates homophily. The assortativities are significantly different for all temperatures from random or heterophilous (P<0.001, t-test comparing with Random). **Right:** Figure 5(b) shows the distribution of reasoning across categories for the networks of Principle 3 (cf. Figure 6). The classification uses GPT-3.5 on a set of 20 randomly sampled reasons repeated over 5 times (frequencies are micro-averaged). The error bars correspond to 95% confidence intervals.

Random), suggesting LLMs' tendency of triadic closure (since an LLM which is given the common neighbors as features should ideally create links within the same community).

Additionally, we observe a statistically significant increase in the marginal transitivity D for all temperatures (P < 0.001, t-test). Moreover, in all cases, the marginal transitivity D is statistically significant compared to Random (P < 0.001, t-test).

These results suggest that the LLM agents exhibit triadic closure. Similar to the approach in earlier reasoning analysis, we present the most common reasons provided by LLMs in Figure  $4^6$ . We find that most of the agents base their decisions on the number of mutual friends.

*Principle 3:* Homophily. Homophily reflects the tendency for nodes with similar characteristics or attributes to form connections and associate with each other. This phenomenon is based on the principle that individuals in a network are more likely to connect with others who share similar traits, interests, or demographics [44].

To test whether LLM agents exhibit homophily, we perform the following experiment: We generate nodes with randomly generated attributes regarding a hobby (randomly chosen among three hobbies), a favorite color (randomly chosen among three colors), and a location within the US (randomly chosen among three US locations) and provide the attributes of the other nodes and the node's own attributes, and each node is tasked to form up to  $\delta = 5$  links with others. For each node i, we provide it with the features  $x_j$  of all non-neighbors j of i. The seed network is taken to be the empty graph.

We run ten simulations for networks with n=50 nodes and  $\delta=5$ . We compare with the Random null model, which chooses  $\delta=5$  links at random.

To measure the presence of homophily, we measure the attribute assortativity coefficient of each of the three features (hobby, color, location). For a property P which takes K distinct values  $P_1, \ldots, P_K$ , its assortativity coefficient R is defined as

<sup>&</sup>lt;sup>6</sup>We do not provide the distribution of reasons for the results of Figure 3(b) as all of the LLM's decisions are made given the number of common neighbors information.

$$R = \frac{\sum_{i=1}^{n} M_{ii} - \sum_{i=1}^{n} a_{i}b_{i}}{1 - \sum_{i=1}^{n} a_{i}b_{i}},$$

where M is the mixing matrix with entries  $M_{ij}$  corresponding to the fraction of edges where one end has value  $P_i$ , and the other end has value  $P_j$ ,  $a_i = \sum_{j=1}^n M_{ij}$  and  $b_i = \sum_{j=1}^n M_{ji}$ . The assortativity has values between -1 and +1, where a positive value denotes the tendency of the nodes to connect to other similar nodes (hence yielding a homophilous network), and a negative value corresponds to connecting to the tendency to connect to dissimilar nodes (which indicates heterophily).

In Figure 5, we observe a consistent pattern of positive assortativity across all temperature ranges, which is higher for lower temperatures. Moreover, the observed assortativity at all temperatures significantly deviates from Random, which has assortativity close to 0 (P < 0.001, t-test comparing with Random). Taken together, we conclude homophily emerges for the networks generated by LLMs.

Moreover, we present the probability of each reason being mentioned in Figure 5. We find that shared hobbies appear to be much more important than shared location or favorite color. This is consistent with our intuition that, similarly to humans, LLMs care more about hobbies than other superficial attributes when forming social connections.

# 3.2 Macro-Level Principles

*Principle 4: Community Structure.* The community structure of networks refers to the organization of nodes or individuals within a network into distinct and densely interconnected groups or clusters [9, 19, 48, 49]. Identifying community structures is crucial for understanding the overall dynamics of a network, as it reveals patterns of relationships and interactions that might not be apparent at the global level.

We seek to examine how triadic closure and homophily contribute to the formation of community structures in networks generated by LLMs. We use the results presented in Section 3.1 to determine whether community structure in networks generated by LLMs emerges from triadic closure or homophily.

First, we consider the networks generated in Figure 3. We examine how LLM agents' choices strengthen the network's community structure. Specifically, we leverage the fact that the SBM graph has a preexisting community structure and measure how the newly formed links reinforce such a structure. Visual inspection shows that the newly added links, represented by the bold edges, happen mostly within each cluster, reinforcing the community structure. This is further quantitatively verified by the fraction  $\hat{p}$  newly created inter-community edges. We find that  $\hat{p}$  is significantly higher than 0.5 (P < 0.001, t-test comparing with 0.5). This indicates that most edges are within the same community, strengthening the community structure.

Next, we use modularity maximization [9] to examine the community structure that arises due to homophily. Intuitively, the modularity measure compares the number of edges inside a community with the expected number of edges that one would find in the cluster if the network were a random network with the same number of nodes and where each node keeps its weighted degree, but edges are otherwise randomly attached according to the Chung-Lu model [18]. This random null model implicitly assumes that each node can attach to another network node. Formally, for a graph with weights  $w_{ij}$  on its edges, the weighted modularity Q [19] of a partition with C communities given by

$$Q = \sum_{c=1}^{C} \left[ \frac{L_c}{W} - r \left( \frac{k_c}{2W} \right)^2 \right],$$

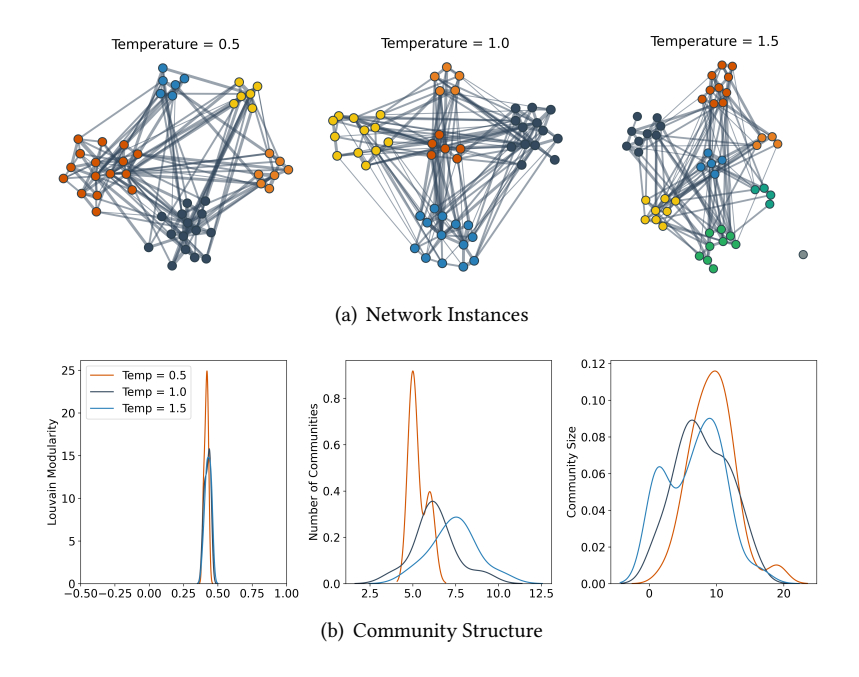


Fig. 6. **Top:** Networks created based on Principle 3. Each node can form at most  $\delta=5$  links with the other nodes based on their attributes. The edge widths correspond to the number of common attributes shared between the nodes. We report the probability of forming a link as a function of the number of common attributes between two nodes. The node colors correspond to the communities found by running the Louvain algorithm. **Bottom:** Louvain modularity, number of communities, and community sizes of networks created based on Principle 3. Lower temperatures yield higher modularity (P<0.001, t-test) and fewer and larger communities (P<0.001, t-test). For smaller temperatures, the communities are more "well-separated".

Here W is the sum of all weights,  $L_c$  is the total weight of intra-community links for community c,  $k_c$  is the total weighted degree of the nodes in the community c and r is the resolution parameter which (we take r=1 from now on). A large positive value (such as greater than 0.5) of the modularity corresponds to evidence of community structure, corresponding to deviation from the random null model. Maximizing Q is NP-Hard, we use the Louvain algorithm [9] to get a lower bound on the maximum modularity.

In Figure 6, we plot the communities found from the Louvain algorithm for the various temperatures, and the Louvain modularity values averaged over ten simulations with 95% confidence intervals. As weights for the network, we use the number of common attributes shared between each pair of nodes, i.e.,  $w_{ij} = \left| \left\{ k : x_i^{(k)} = x_j^{(k)} \right\} \right|$  for each link (i,j) in the final network, where  $x_i^{(k)}$  and  $x_j^{(k)}$  correspond to the k-th features of  $x_i$  and  $x_j$ , respectively. We find that for all temperatures, the Louvain partitions exhibit community structure which corresponds to positive modularity (P < 0.001, t-test) compared to the modularity Q = 0 of the random graph), which is most concentrated for smaller temperatures, and that as the temperature increases, the Louvain modularity increases (P < 0.001, t-test). Also, the smaller the temperature, the fewer (and larger) on-average communities the Louvain algorithm finds (P < 0.001, t-test). Finally, the communities tend to be visually more "separated" for lower temperatures. We argue that this is because higher temperatures indicate more randomness in the decisions.

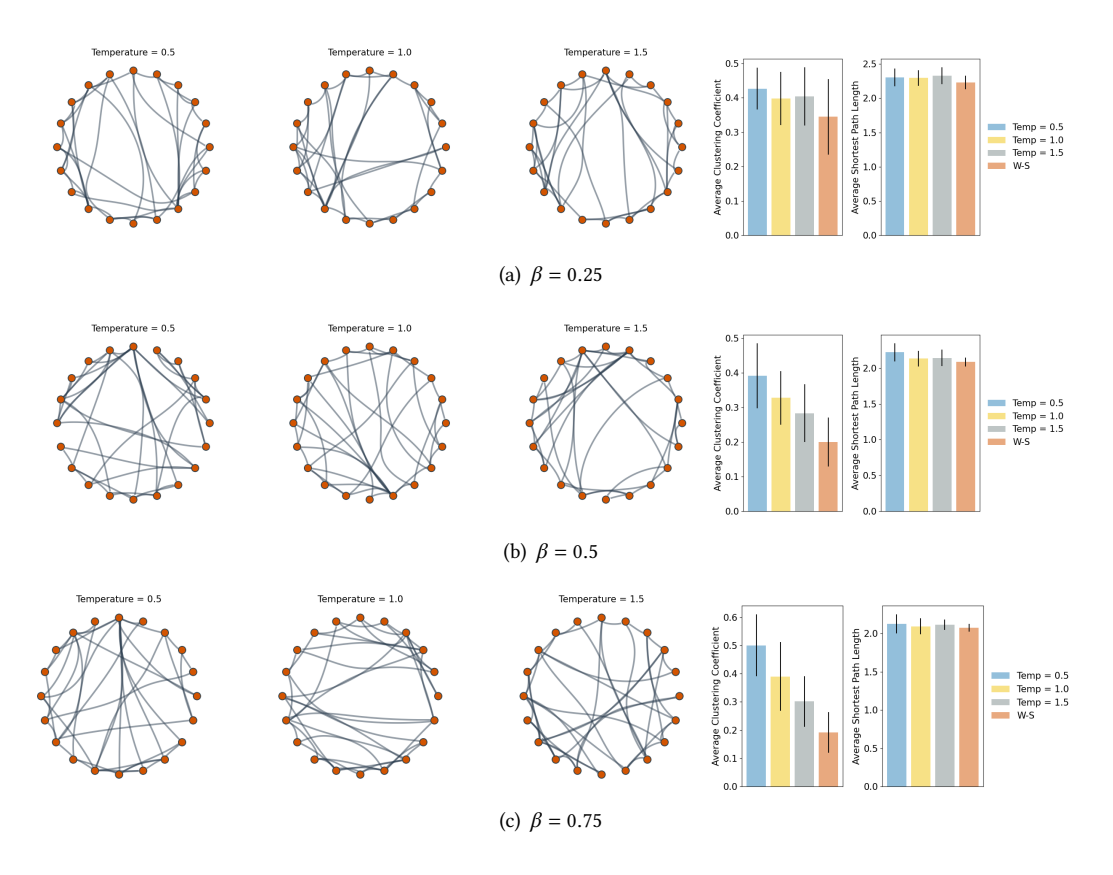


Fig. 7. Networks and distribution of reasoning created based on Principle 5 using the altered Watts-Strogatz Model for  $n = 50, k = 5, \beta \in \{0.25, 0.5, 0.75\}$ , together with plots of the average clustering coefficient C and the average shortest path length L. The comparison is made with respect to a Watts-Strogatz graph with  $n = 50, k = 5, \beta \in \{0.25, 0.5, 0.75\}$ . In most cases we observe strong evidence that  $L \sim \log(n)$  and  $C \sim 1/\log(n)$ .

Our results indicate that community structure emerges in networks generated by LLMs. Namely, the networks generated by LLMs obey triadic closure, and as a result, the community structure is reinforced. Moreover, networks generated by LLMs are also homophilous, allowing community structure to emerge. Finally, in Section 3.3, we show that the community structure is reinforced in real-world networks where LLMs take a variety of factors, such as homophily and triadic closure jointly into account in their choices of whom to form a link with.

*Principle 5: Small-World.* The small-world phenomenon in networks [34, 63] refers to the principle where most nodes in a network are only a few connections away from each other despite the network's large size. In a small-world network, there is a delicate balance between local clustering and short average path lengths: Nodes tend to form clusters or groups (triadic closure), exhibiting a high level of interconnectedness within these local neighborhoods, whereas at the same time, the existence of a few long-range connections ensures that the entire network is reachable with relatively few steps [32, 42, 54].

Formally, a small-world network is a network where the *average shortest path length* L grows proportionally to the network size n, namely

### $L \sim \log(n)$ ,

while the average clustering coefficient is not small [63]. One of the models shown to exhibit the "small-world" phenomenon is the Watts-Strogatz model [63], which we use as a basis for our analysis below. Empirical work has shown that many real-world organizational networks that exhibit the small-world phenomenon have an average shortest path length L that varies as  $\log(n)$  and the average clustering coefficient C varies as  $C \sim 1/\log(n)$  [31].

To investigate whether LLMs can generate networks that exhibit the small-world phenomenon, we employ a stochastic process analogous to the Watts-Strogatz model [63] and then fit regression models for the average shortest path length and the average clustering coefficient. This approach allows for a direct comparison of the emergence of small-world properties, such as decreasing average path lengths and increasing clustering coefficients, with those observed in the Watts-Strogatz model, which serves as a null model. The generation process is parametrized by three numbers: the number of nodes n, the number of long-range connections k, and the rewiring probability  $\beta$ . The algorithm proceeds as follows:

- (1) Similarly to Watts-Strogatz, we first create a ring network with n nodes. After that, for each node [n], we create k edges where k/2 edges connect to its rightmost neighbors and k/2 edges connect to its leftmost neighbors.
- (2) To create  $G_t$ , for each node [n], we take its k/2 rightmost neighbors and rewire them with probability  $\beta$ . For each of the k/2 rightmost neighbors that are to be rewired, we make one query to the LLM, which indicates how the edge will be rewired. The choice is made by providing the LLM with all the network nodes and each node's neighbors (i.e., the network structure).

The model closely resembles the Watts-Strogatz model, with the primary distinction being the method of edge rewiring. Instead of randomly selecting edges for rewiring, as in the Watts-Strogatz model, we determine the rewiring of an edge by inquiring about the LLM and providing it with the current network structure.

To test the relation of the average shortest path length and the average clustering coefficient with n and compare with the results reported in [31], we create networks of various sizes from n=10 to n=100 and Figure 8 for  $\beta \in \{0.25, 0.5, 0.75\}$  and k=5. Some instances of these networks are shown in Figure 7 We run regressions relating to the average shortest path length with  $\log(n)$  and observe that for all temperatures, we obtain statistically significant results (see the significance indicators in Figure 8, where most regressions have P < 0.001) being that the average shortest path length scales proportionally to  $\log(n)$  per existing works [31]. Similarly, we show that the average clustering coefficient scales as  $1/\log(n)$  (again, most regression results have P < 0.001), in agreement with [31].

While we have shown that we have strong evidence that  $L \sim \log(n)$  and  $C \sim 1/\log(n)$  for the networks of Figures 7 and 8 indicating small-world properties do exist, we have not identified whether these networks have similar statistics with the actual Watts-Strogatz model. Specifically, as Figure 7 shows, we obtain weak evidence that the final generated networks have the similar average shortest path length as Watts-Strogatz with  $\beta \in \{0.25, 0.5, 0.75\}$  (P < 0.1, t-test comparing the resulting average shortest path lengths of the networks generated by multi-LLMs and the Watts-Strogatz average shortest path lengths for  $\beta \in \{0.25, 0.5, 0.75\}$ ) and a larger average clustering coefficient than Watts-Strogatz (P < 0.1, t-test comparing the resulting average clustering coefficient of the networks generated by multi-LLMs and the Watts-Strogatz average clustering coefficient for  $\beta \in \{0.25, 0.5, 0.75\}$ ).

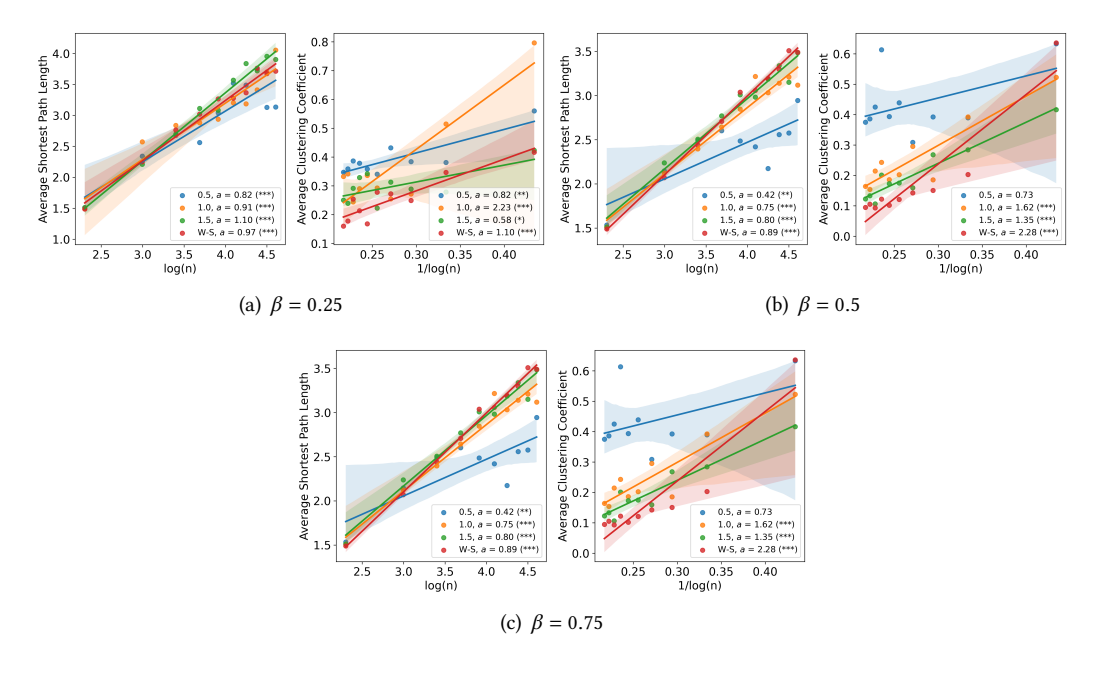


Fig. 8. Regression plots relating average shortest path length and average clustering coefficient with n for  $\beta \in \{0.25, 0.5, 0.75\}$  and k = 5. a represents the slope of the regression lines. \* indicates P < 0.05, \*\* indicates P < 0.01, and \*\* indicates P < 0.001.

This raises the following question: Does a value  $\hat{\beta} \neq \beta$  exist such that Watts-Strogatz networks generated with rewiring probability  $\hat{\beta}$  "resemble" the LLM-generated networks? To find such values  $\hat{\beta}$ , we do a binary search on  $\hat{\beta}$  such that the average clustering coefficient of a Watts-Strogatz network with rewiring probability  $\hat{\beta}$  matches the empirical average clustering coefficient of the LLM-generated network. In Figure 9, we plot the estimated values for  $\hat{\beta}$  for each value of  $\beta$ , each simulation and each temperature. Additionally, we plot the average shortest path length difference between the Watts-Strogatz graph generated having rewiring probability  $\hat{\beta}$  for each simulation and the LLM-generated networks. To this end, we observe that, although not identical, the two quantities are close to each other. Specifically, a t-test comparing with the average shortest path length of Watts-Strogatz with rewiring probability  $\hat{\beta}$  yields P > 0.1 for all temperatures for  $\beta = 0.25$ , and P > 0.1 for the temperatures being 0.5 and 1.5 and 0.05 < P < 0.1 for the temperature being 1.0 for  $\beta \in \{0.25, 0.75\}$ .

These results suggest that LLMs do exhibit small-world properties. Specifically, the average shortest path length scales as  $\log(n)$ , and the average clustering coefficient scales as  $1/\log(n)$ , which are considered important statistical properties of small-world networks by [31]. Moreover, these networks have similar (though not identical) average shortest path lengths with Watts-Strogatz networks with rewiring probabilities  $\hat{\beta} \neq \beta$ .

#### 3.3 Real-World Networks

To understand the behavior of LLMs in the context of real-world network formation, we utilize the *Facebook100* dataset [59] and a discrete choice modeling framework [43, 51]. The dataset consists of "friendship" networks at one hundred American colleges and universities at a single point in

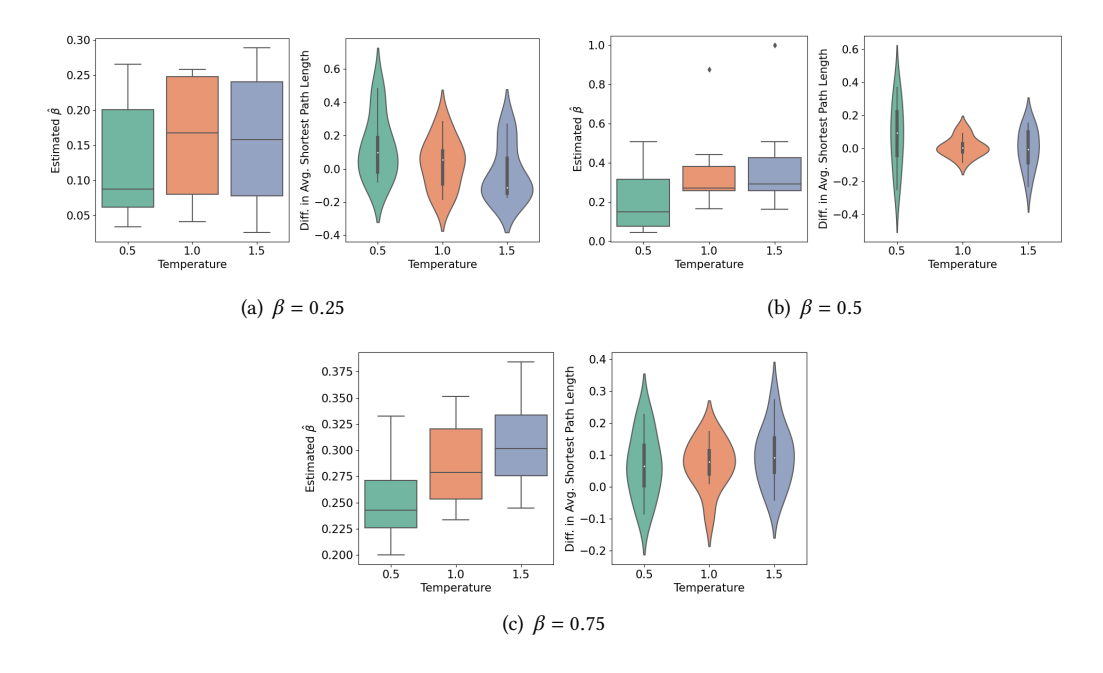


Fig. 9. Estimated values  $\hat{\beta}$  of  $\beta \in \{0.25, 0.5, 0.75\}$  for LLM-generated networks based on matching the average clustering coefficient and difference in the average shortest path between LLM-generated networks and Watts-Strogatz with rewiring probability  $\hat{\beta}$ .

time from Facebook's online social network. We model the network formation process as a discrete choice process in which nodes are sequentially asked to form links from a set of alternatives.

Discrete Choice Model. For each node i that we consider at time t, we randomly remove one of its current friends from the real-world network. Subsequently, we present each node with a set of candidate nodes (denoted by  $A_t$ ), comprising one of the removed friends and other nodes that were not originally its friends. We then instruct the LLM to form a link with one of the candidates, providing the attributes of the candidates and the social network structure to aid its decision-making. These choices are made sequentially.

We use the *utility* of the model for each node for each sequential decision of network formation:

$$U_{ij,t} = \theta_{PA} \log d_{i,t} + \theta_{H} \log w_{ij} + \theta_{TC} \log c_{ij,t} + \epsilon_{ij,t},$$

In this equation,  $\theta_{PA}$  measures the strength of preferential attachment based on the degree  $d_{j,t}$  of j at step t,  $\theta_H$  measures the strength of homophily based on the similarity  $w_{ij}$  (i.e. number of common attributes) between i and j, and  $\theta_{TC}$  measures the strength of triadic closure, based on the number of common neighbors  $c_{ij,t}$  between i and j at step t. The error term  $\epsilon_{ij,t}$  is distributed as i.i.d. standard Gumbel<sup>7</sup>. The covariates are range-normalized.

The multinomial logit model (MNL) indicates that the probability that i links to j at step t is given by

<sup>&</sup>lt;sup>7</sup>The standard Gumbel distribution has CDF  $e^{e^{-x}}$ .

Temp.	$\hat{ heta}_{ ext{PA}}$	$\hat{ heta}_{ m H}$	$\hat{ heta}_{ ext{TC}}$	LL	AIC	% Change Acc.	% Change $L$	% Change C	$\Delta Q$ (t-stat)
		Caltech36 (769 nodes, 33,312 edges)							
0.5 1.0	0.41*** (0.31) 0.36*** (0.13)	1.95*** (0.64) 1.85*** (0.52)	0.59*** (0.37) 0.58*** (0.33)	-1,377.47 -1.435.07	2,762.94 2.878.13	171.8 179.6	-0.008 -0.18	-9.94 -11.08	3.45** 3.49**
1.5	0.36*** (0.16)	1.72*** (0.31)	0.55*** (0.20)	-1,522.47	3,052.94	127.6	-0.06	-11.46	3.37**
		Swarthmore42 (1,659 nodes, 12,2100 edges)							
0.5 1.0	0.18*** (0.13) 0.26*** (0.07)	1.62*** (0.23) 1.70*** (0.35)	0.65*** (0.08) 0.58*** (0.12)	-2,838.33 -2,927.99	5,684.66 5,863.97	124.2 91.6	0.01 -0.10	-11.46 -4.25	7.42*** 1.96*
1.5	0.19*** (0.14) 1.50*** (0.33) 0.59*** (0.10) -3,139.42 6,286.83 87.39 -0.20 -4.52 4.03***  UChicago30 (6,591 nodes, 416,206 edges)								
0.5 1.0 1.5	0.23*** (0.06) 0.23*** (0.10) 0.22*** (0.12)	2.00*** (0.24) 1.98*** (0.17) 1.78*** (0.27)	0.41*** (0.09) 0.38*** (0.06) 0.41*** (0.07)	-3,444.33 -3,578.18 -2,033.49	6,896.67 7,164.36 4,074.98	217.2 219.2 222.4	-0.24 -0.12 -0.17	-2.52 -2.66 -2.42	7.46*** [0.34] 9.56*** [1.05] 10.19*** [0.24]

Notes  $\hat{\theta}_{\text{PA}} = \text{Coefficient of log degree}, \ \hat{\theta}_{\text{H}} = \text{Coefficient of log \# of common attributes}, \ \hat{\theta}_{\text{TC}} = \text{Coefficient of log \# common neighbors}$  LL = Log-likelihood, AIC = Akaike Information Criterion  $\text{Acc.} = \text{Accuracy, } L = \text{Average Path Length, } C = \text{Average Clustering Coefficient, } \Delta Q \text{ (t-stat)} = \text{Modularity change t-statistic}$   $^*: P < 0.05, \ ^{**}: P < 0.01, \ ^{***}: P < 0.001$ 

Table 1. Multinomial logit coefficients for three networks from the Facebook 100 dataset. The standard errors of the estimates are shown in parentheses. The full regression tables can be found in Appendix A. The null hypothesis corresponds to the respective parameter being equal to 0. We report the percent change in accuracy, average path length, and average clustering coefficient compared to the initial network (before the deletion of edges). For the change in modularity, we run the Louvain algorithm ten times and perform a t-test with the resulting modularities. For the UChicago 30 dataset, we report the t-statistic value in the subgraph induced by the 2,000 sampled nodes. We also report the modularity change (t-statistic) in the whole graph inside brackets.

$$p_{ij,t} = \Pr\left[\operatorname{argmax}_{r \in A_t} U_{ir,t} = j\right] = \frac{d_{j,t}^{\theta_{\text{PA}}} w_{ij}^{\theta_{\text{H}}} c_{ij,t}^{\theta_{\text{TC}}}}{\sum_{r \in A_t} d_{r,t}^{\theta_{\text{PA}}} w_{ir}^{\theta_{\text{H}}} c_{ir,t}^{\theta_{\text{TC}}}}$$

Given a sequence of nodes  $i_1, \ldots, i_T \in V$  and choices (denoted by subscripted j)  $j_1 \in A_1, \ldots, j_T \in A_T$ , the parameters can be found by maximizing the log-likelihood function. To get the standard errors of the coefficients and the corresponding P-values, we follow the process outlined in [51].

Experiment Setup and Rationale. We use datasets that refer to three US colleges – Caltech36, Swarthmore42, and UChicago30. They represent different sizes of networks: n = 769, n = 1,659, and n = 6,591 nodes, respectively.

After the removal procedure we described, we obtain the initial network  $G_1$ . For the Caltech36 (n = 769) and Swarthmore42 (n = 1,659) datasets, we consider all of the nodes of the networks as nodes that have to make a choice. For the UChicago30 dataset, we consider a randomly sampled subset of 2,000 nodes because of the limited context window of GPT models. We set the size of the alternative sets to 20, and thus, the accuracy of random guessing is 5%.

Regression Results and LLM-based Reasoning. We present the regression results in Table 1. Our analysis reveals that the degree, the number of common neighbors, and the number of shared interests are all statistically significant factors influencing the choices of LLMs (P < 0.001) across all datasets. Furthermore, we find that LLMs place the greatest emphasis on the number of common attributes ( $\hat{\theta}_{\rm H}$ ), followed by the number of common neighbors ( $\hat{\theta}_{\rm TC}$ ), and then the degree ( $\hat{\theta}_{\rm PA}$ ).

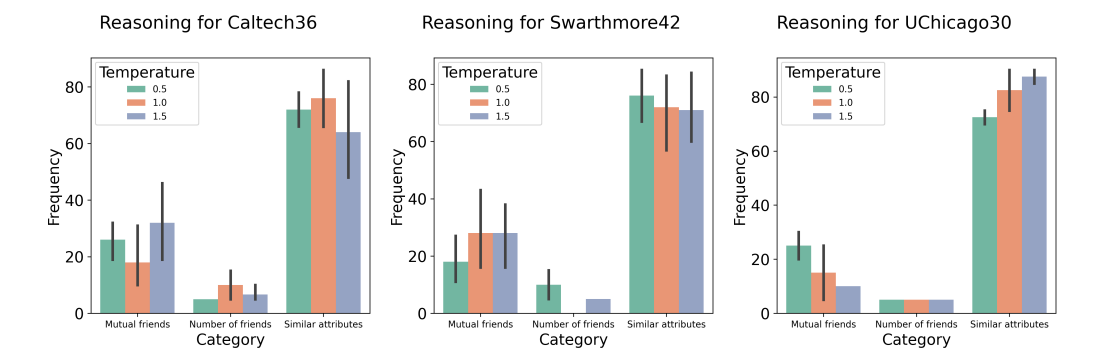


Fig. 10. Distribution of reasoning across categories for the real-world networks. The classification is done using GPT-4 on a set of 20 randomly sampled reasons repeated over 5 times. In agreement with Table 1, the multi-LLMs put more weight on homophily, then on triadic closure, and then on preferential attachment. The error bars correspond to 95% confidence intervals.

These results suggest that LLMs exhibit a strong preference for homophily, followed by a tendency towards triadic closure, and finally, preferential attachment. Specifically, the relationship  $\hat{\theta}_{\rm H} > \hat{\theta}_{\rm TC} > \hat{\theta}_{\rm PA}$  holds across all examined datasets and temperature settings.

Moreover, Figure 10 demonstrates that the reasoning provided by LLMs aligns with the aforementioned findings. In particular, LLMs emphasize homophily, indicating that nodes sharing similar characteristics—such as student/faculty status, high school, and graduation year—are more likely to form connections. Conversely, the effects of triadic closure and preferential attachment are less prominent.

In summary, our analysis indicates that although preferential attachment, homophily, and triadic closure are all present in the network formation behaviors of LLMs, homophily emerges as the predominant driving force.

Percent Increase in Accuracy Compared to Random Guessing. We evaluate the percentage increase in accuracy, where accuracy is defined as the likelihood of selecting a previously existing neighbor from a set of alternatives, compared to making a random selection from 20 possible options. As shown in Table 1, LLMs demonstrate a substantially higher accuracy in their selections than would be expected from random guessing.

Average Shortest Path Length. We measure the percent change in the average shortest path length between the network before the edge deletions and the network after the choices made by the LLM agents (see Table 1). We observe a small decrease in the average path length in the new network in almost all cases indicating that the average shortest path length decreases slightly, indicating strengthening of the small-world phenomenon.

*Triadic Closure.* In addition to the coefficient  $\hat{\theta}_{TC}$  of triadic closure, we measure the percent change in the average shortest path length and the average clustering coefficient between the network before the edge deletions and the network after the choices made by the LLM agents (see Table 1). We observe that the average clustering coefficient also decreases compared to the initial network, indicating the weakening of triadic closure compared to the initial network.

*Community Structure.* We run the Louvain algorithm 10 times for both the initial graph  $G_1$  and the final graph  $G_T$  and perform a t-test between the resulting modularities (see Table 1). We observe

that the modularity increases in all cases and is statistically significant. This suggests that LLMs make choices that naturally yield a reinforcement of the community structure.

#### 4 RELATED WORK

In this section, we review the following collections of literature on networks and LLMs: (i) classical models in network science, (ii) concurrent works at the intersection between networks and LLMs, and (iii) broad applications of LLMs to social sciences.

### 4.1 Classical Network Formation Models

Here we review the literature on network formation models.

The Barabási–Albert (BA) model [7] is among the most well-known science models. It describes the "the-rich-get-richer" effect regarding network connections using minimal assumptions, including preferential attachment. Although our study only examines the BA model, this stream has multiple extensions. For example, the fitness model – or Bianconi-Barabási model – [8] where nodes form new links proportionally to each alternative's fitness, the generalized preferential attachment model. Chung-Lu model [18] creates random networks from a prescribed degree sequence. Geometric preferential attachment models [10, 11, 22] combine preferential attachment with geometric constraints.

As for homophily, triadic closure, and community structure in networks, there has been a significant amount of research has been devoted to studying stochastic blockmodels [1, 28] that combines these three. The stochastic block model is a random graph model with a community structure. To this end, our study uses stochastic block models as the basic networks upon which the LLMs make choices, showing that triadic closure and community structure emerge in networks generated by LLMs, which are similar to real-world networks [25, 46]. Moreover, our paper utilizes modularity maximization methods [9, 48, 49] to recover communities in the networks generated by multi-LLMs.

The Watts-Strogatz model is characterized by short average shortest path lengths and high clustering coefficients [34, 63]. It explains the "small-world phenomenon," which means the average distance between any two people is short (in fact, logarithmic in the network size) [60]. Recently, it has been observed in [31] that real-world organizational networks have logarithmic average shortest path lengths and clustering coefficients that vary inversely with the logarithm of the number of nodes. Our work contributes to this line of work by designing a multi-LLM-based random graph model that exhibits logarithmic average shortest path lengths and a clustering coefficient that varies inversely with the logarithm of the size of the network consistent to small-world networks.

Finally, our study treats the choices made by multi-LLMs in real-world network scenarios (cf. Section 3.3) as a discrete choice modeling problem where each agent's utility is modeled after a homophily, a triadic closure, and a preferential attachment term as these are the main micro-level principles that emerge in networks simulated by multi-LLMs. To this end, we mention that treating network growth as a discrete choice modeling problem in classical network science problems has been studied in [51]. Our work leverages techniques from the work of [51] to fit discrete choice models to model the choices made by LLM-based agents (contrary to real-world networks that the work of [51] studies).

### 4.2 Existing studies on networks and multi-LLMs

Our study serves as the first comprehensive examination of social networking behavior in LLMs. While a few studies have explored one or a few aspects of networking behavior in LLMs, our research provides a more holistic view.

For example, [20] exclusively examines the emergence of the preferential attachment mechanism in networks simulated by LLM-based agents. However, their study only provides degree information rather than network structure, and they observe a "star-like" network where only one central node receives all the connections. This observation aligns with our discussion in Figure 1(b). In contrast, we find that providing LLMs with the topology of the network (i.e., each agent's neighbors) allows us to recover networks that follow a power-law degree distribution, which, in some cases, are identical to the BA model (cf. Figure 1(a)).

Concurrently, [27] examines how LLMs interact in human-like societies by conducting a sandbox experiment on a social network platform. The authors show that homophily patterns emerge between the agents similarly to humans. However, our study not only examines multiple aspects of network formation in addition to homophily but also compares the strengths of different drivers.

Moreover, [53] designs interactive environments among multiple LLMs with synthesized memories and dynamic planning. Similarly, the works of [38] and [64] leveraged LLMs to simulate complex social interactions such as collaboration, coordination, exchange, and competition and observed the emergence of such phenomena. However, they did not explicitly examine the network formation behavior of LLMs.

Finally, [24] introduces the  $S^3$  system, where LLMs are emulated similarly to a real human society (with emotions, attitudes, and interactions) and observe the emergence of phenomena that exist in human societies. Relevantly, [33] presents Social-LLM and proposes a user modeling approach based on social network data and large language models focusing on detection tasks. However, our focus is on the emergence of network principles in contrast to social simulations or detection tasks.

### 4.3 Broad literature on understanding the behavior of LLMs in social science contexts

Our study contributes to the emerging field of understanding LLMs' behavior in social science contexts. While the computer science literature has extensively examined LLMs from multiple perspectives, including bias and fairness [40], understanding how LLMs' behaviors mirror human behaviors from a social science standpoint remains limited.

Recent studies have explored various aspects of LLMs' behavior, such as rationality [15], social preferences [29, 37], social learning [37], strategic thinking [3, 14], the diffusion of ideas and opinions [17], and cooperation and coordination [21, 52]. Furthermore, research in psychology has sought to understand the personality and values of LLMs, as demonstrated by studies [45] and [55].

These investigations provide valuable insights into LLMs' behavior, offering opportunities to employ LLMs for social simulations or agent-based modeling and to undertake efforts in model alignment. The ongoing work in this area, including studies [24, 26, 39, 53], highlights the potential for paradigm shifts in social science studies and a deeper understanding of human-AI interactions.

By synthesizing these insights, our research aims to contribute to the broader conversation on LLMs in social contexts, emphasizing the importance of understanding both human and AI behaviors and their interactions. This approach enriches our comprehension of LLMs and opens new avenues for interdisciplinary research in social sciences and artificial intelligence.

### 5 DISCUSSION

Our study conducted a comprehensive evaluation of LLMs' network formation preferences, encompassing both micro-level network principles such as preferential attachment, triadic closure, and homophily and macro-level network principles like community structure and the small-world phenomenon. Our findings indicate that networks generated by multiple LLMs do exhibit these properties, particularly when primed with network statistics such as the number of mutual friends or the degree of alternatives.

Furthermore, through discrete choice modeling, we explored the emergence of these properties in real-world networks. Our results reveal that the agents' selections are predominantly driven by homophily, followed by triadic closure, and then preferential attachment. Additionally, we observed a strengthening of community structure in real-world network experiments.

Our study enhances our understanding of the behavior of LLMs. For example, our findings reveal varying strengths of network formation properties, suggesting that when LLMs are employed to coordinate social networks in social or work environments, they may exhibit behaviors similar to humans. This insight contributes to developing socially aware LLMs that align with human preferences, with potential applications ranging from chatbots and virtual assistants to collaborative systems and social media platforms.

Furthermore, our research provides valuable insights into network science by exploring how LLMs can be utilized in network science studies. As LLMs possess fundamental network principles and exhibit human-like network formation behaviors, their use in simulations of social systems or agent-based modeling holds great promise. This advancement aids in the further development of social science studies, particularly in the areas of network formation and social dynamics.

Looking ahead, we propose two promising directions for future research. First, we propose investigating LLM behavior in more complex interactions, such as simulated dialogs or specific environments like companies, schools, or parties. By examining LLMs in these contexts, we can better understand their network formation preferences and how they adapt to different social dynamics. This research could shed light on the nuances of LLM behavior in realistic settings and inform their integration into diverse social environments.

Second, we suggest exploring the application of our findings in specific settings, particularly in organizational contexts. For example, considering the potential use of LLMs to assist HR professionals, our study's insights could guide the alignment of LLMs with organizational goals. By leveraging network information, LLMs could help HR departments identify their firms' best fit or talent, optimizing recruitment and talent management processes.

### **ACKNOWLEDGMENTS**

M.P. is supported by a scholarship from the Onassis Foundation (Scholarship ID: F ZT 056-1/2023-2024).

#### REFERENCES

- [1] Emmanuel Abbe. 2018. Community detection and stochastic block models: recent developments. *Journal of Machine Learning Research* 18, 177 (2018), 1–86.
- [2] Gati V Aher, Rosa I Arriaga, and Adam Tauman Kalai. 2023. Using large language models to simulate multiple humans and replicate human subject studies. In *International Conference on Machine Learning*. PMLR, 337–371.
- [3] Elif Akata, Lion Schulz, Julian Coda-Forno, Seong Joon Oh, Matthias Bethge, and Eric Schulz. 2023. Playing repeated games with Large Language Models. *arXiv preprint arXiv:2305.16867* (2023).
- [4] Eytan Bakshy, Itamar Rosenn, Cameron Marlow, and Lada Adamic. 2012. The role of social networks in information diffusion. In Proceedings of the 21st international conference on World Wide Web. 519–528.
- [5] Abhijit Banerjee, Arun G Chandrasekhar, Esther Duflo, and Matthew O Jackson. 2013. The diffusion of microfinance. Science 341, 6144 (2013), 1236498.
- [6] Albert-László Barabási. 2013. Network science. Philosophical Transactions of the Royal Society A: Mathematical, Physical and Engineering Sciences 371, 1987 (2013), 20120375.
- [7] Albert-László Barabási and Réka Albert. 1999. Emergence of scaling in random networks. Science 286, 5439 (1999), 509-512.
- [8] Ginestra Bianconi and A-L Barabási. 2001. Competition and multiscaling in evolving networks. *Europhysics letters* 54, 4 (2001), 436.
- [9] Vincent D Blondel, Jean-Loup Guillaume, Renaud Lambiotte, and Etienne Lefebvre. 2008. Fast unfolding of communities in large networks. Journal of statistical mechanics: theory and experiment 2008, 10 (2008), P10008.

- [10] Anthony Bonato, Jeannette Janssen, and Pawel Prałat. 2010. The geometric protean model for on-line social networks. In Algorithms and Models for the Web-Graph: 7th International Workshop, WAW 2010, Stanford, CA, USA, December 13-14, 2010. Proceedings 7. Springer, 110–121.
- [11] Anthony Bonato, Jeannette Janssen, and Paweł Prałat. 2012. Geometric protean graphs. Internet Mathematics 8, 1-2 (2012), 2-28.
- [12] Shikha Bordia and Samuel R Bowman. 2019. Identifying and reducing gender bias in word-level language models. arXiv preprint arXiv:1904.03035 (2019).
- [13] Stephen P Borgatti and Martin G Everett. 2000. Models of core/periphery structures. *Social networks* 21, 4 (2000), 375–395.
- [14] Philip Brookins and Jason Matthew DeBacker. 2023. Playing games with GPT: What can we learn about a large language model from canonical strategic games? Available at SSRN 4493398 (2023).
- [15] Yiting Chen, Tracy Xiao Liu, You Shan, and Songfa Zhong. 2023. The Emergence of Economic Rationality of GPT. arXiv preprint arXiv:2305.12763 120, 51 (2023), e2316205120. https://doi.org/10.1073/pnas.2316205120 arXiv:https://www.pnas.org/doi/pdf/10.1073/pnas.2316205120
- [16] Felix Chopra and Ingar Haaland. 2023. Conducting qualitative interviews with AI. (2023).
- [17] Yun-Shiuan Chuang, Agam Goyal, Nikunj Harlalka, Siddharth Suresh, Robert Hawkins, Sijia Yang, Dhavan Shah, Junjie Hu, and Timothy T. Rogers. 2023. Simulating Opinion Dynamics with Networks of LLM-based Agents. arXiv:2311.09618 [physics.soc-ph]
- [18] Fan Chung and Linyuan Lu. 2004. The average distance in a random graph with given expected degrees. *Internet Mathematics* 1, 1 (2004), 91–113.
- [19] Aaron Clauset, Mark EJ Newman, and Cristopher Moore. 2004. Finding community structure in very large networks. *Physical review E* 70, 6 (2004), 066111.
- [20] Giordano De Marzo, Luciano Pietronero, and David Garcia. 2023. Emergence of Scale-Free Networks in Social Interactions among Large Language Models. arXiv preprint arXiv:2312.06619 (2023).
- [21] Sara Fish, Paul Gölz, David C. Parkes, Ariel D. Procaccia, Gili Rusak, Itai Shapira, and Manuel Wüthrich. 2023. Generative Social Choice. arXiv:2309.01291 [cs.GT]
- [22] Abraham D Flaxman, Alan M Frieze, and Juan Vera. 2006. A geometric preferential attachment model of networks. *Internet Mathematics* 3, 2 (2006), 187–205.
- [23] James H Fowler and Nicholas A Christakis. 2008. Dynamic spread of happiness in a large social network: longitudinal analysis over 20 years in the Framingham Heart Study. *Bmj* 337 (2008).
- [24] Chen Gao, Xiaochong Lan, Zhihong Lu, Jinzhu Mao, Jinghua Piao, Huandong Wang, Depeng Jin, and Yong Li. 2023. S3: Social-network Simulation System with Large Language Model-Empowered Agents. arXiv preprint arXiv:2307.14984 (2023)
- [25] Mark S Granovetter. 1973. The strength of weak ties. American journal of sociology 78, 6 (1973), 1360-1380.
- [26] Lewis D Griffin, Bennett Kleinberg, Maximilian Mozes, Kimberly T Mai, Maria Vau, Matthew Caldwell, and Augustine Marvor-Parker. 2023. Susceptibility to Influence of Large Language Models. arXiv preprint arXiv:2303.06074 (2023).
- [27] James He, Felix Wallis, and Steve Rathje. 2023. Homophily in An Artificial Social Network of Agents Powered by Large Language Models. (2023).
- [28] Paul W Holland, Kathryn Blackmond Laskey, and Samuel Leinhardt. 1983. Stochastic blockmodels: First steps. Social Networks 5, 2 (1983), 109–137.
- [29] John J Horton. 2023. Large language models as simulated economic agents: What can we learn from homo silicus? Technical Report. National Bureau of Economic Research.
- [30] Matthew O Jackson. 2008. Social and economic networks. Vol. 3. Princeton university press Princeton.
- [31] Abigail Z Jacobs and Duncan J Watts. 2021. A large-scale comparative study of informal social networks in firms. Management Science 67, 9 (2021), 5489–5509.
- [32] Eaman Jahani, Samuel P Fraiberger, Michael Bailey, and Dean Eckles. 2023. Long ties, disruptive life events, and economic prosperity. *Proceedings of the National Academy of Sciences* 120, 28 (2023), e2211062120.
- [33] Julie Jiang and Emilio Ferrara. 2023. Social-LLM: Modeling User Behavior at Scale using Language Models and Social Network Data. arXiv preprint arXiv:2401.00893 (2023).
- [34] Jon Kleinberg. 2000. The small-world phenomenon: An algorithmic perspective. In *Proceedings of the thirty-second annual ACM symposium on Theory of computing*. 163–170.
- [35] Hadas Kotek, Rikker Dockum, and David Sun. 2023. Gender bias and stereotypes in Large Language Models. In *Proceedings of The ACM Collective Intelligence Conference*. 12–24.
- [36] Yan Leng, Tara Sowrirajan, Yujia Zhai, and Alex Pentland. 2023. Interpretable stochastic block influence model: measuring social influence among homophilous communities. *IEEE Transactions on Knowledge and Data Engineering* (2023).
- [37] Yan Leng and Yuan Yuan. 2023. Do LLM Agents Exhibit Social Behavior? arXiv preprint arXiv:2312.15198 (2023).

- [38] Guohao Li, Hasan Abed Al Kader Hammoud, Hani Itani, Dmitrii Khizbullin, and Bernard Ghanem. 2023. Camel: Communicative agents for mind exploration of large scale language model society. arXiv preprint arXiv:2303.17760 (2023).
- [39] Yuan Li, Yixuan Zhang, and Lichao Sun. 2023. Metaagents: Simulating interactions of human behaviors for llm-based task-oriented coordination via collaborative generative agents. arXiv preprint arXiv:2310.06500 (2023).
- [40] Percy Liang, Rishi Bommasani, Tony Lee, Dimitris Tsipras, Dilara Soylu, Michihiro Yasunaga, Yian Zhang, Deepak Narayanan, Yuhuai Wu, Ananya Kumar, et al. 2022. Holistic evaluation of language models. arXiv preprint arXiv:2211.09110 (2022).
- [41] David Liben-Nowell and Jon Kleinberg. 2003. The link prediction problem for social networks. In *Proceedings of the twelfth international conference on Information and knowledge management*. 556–559.
- [42] Ding Lyu, Yuan Yuan, Lin Wang, Xiaofan Wang, and Alex Pentland. 2022. Investigating and modeling the dynamics of long ties. Communications Physics 5, 1 (2022), 87.
- [43] Daniel McFadden. 1972. Conditional logit analysis of qualitative choice behavior. (1972).
- [44] Miller McPherson, Lynn Smith-Lovin, and James M Cook. 2001. Birds of a feather: Homophily in social networks. Annual review of sociology 27, 1 (2001), 415–444.
- [45] Marilù Miotto, Nicola Rossberg, and Bennett Kleinberg. 2022. Who is GPT-3? an exploration of personality, values and demographics. arXiv preprint arXiv:2209.14338 (2022).
- [46] Mohsen Mosleh, Dean Eckles, and David Gertler Rand. 2024. *Tendencies toward triadic closure: Field-experimental evidence*. Technical Report. Center for Open Science.
- [47] Mark EJ Newman. 2003. Mixing patterns in networks. Physical review E 67, 2 (2003), 026126.
- [48] Mark EJ Newman. 2006. Modularity and community structure in networks. *Proceedings of the national academy of sciences* 103, 23 (2006), 8577–8582.
- [49] Mark EJ Newman and Michelle Girvan. 2004. Finding and evaluating community structure in networks. *Physical review E* 69, 2 (2004), 026113.
- [50] OpenAI. 2023. GPT-4 technical report. arXiv (2023), 2303-08774.
- [51] Jan Overgoor, Austin Benson, and Johan Ugander. 2019. Choosing to grow a graph: Modeling network formation as discrete choice. In The World Wide Web Conference. 1409–1420.
- [52] Marios Papachristou, Longqi Yang, and Chin-Chia Hsu. 2023. Leveraging Large Language Models for Collective Decision-Making. arXiv preprint arXiv:2311.04928 (2023).
- [53] Joon Sung Park, Joseph C O'Brien, Carrie J Cai, Meredith Ringel Morris, Percy Liang, and Michael S Bernstein. 2023. Generative agents: Interactive simulacra of human behavior. arXiv preprint arXiv:2304.03442 (2023), 1–22.
- [54] Patrick S Park, Joshua E Blumenstock, and Michael W Macy. 2018. The strength of long-range ties in population-scale social networks. *Science* 362, 6421 (2018), 1410–1413.
- [55] Max Pellert, Clemens M Lechner, Claudia Wagner, Beatrice Rammstedt, and Markus Strohmaier. 2023. AI Psychometrics: Using psychometric inventories to obtain psychological profiles of large language models. (2023).
- [56] Iyad Rahwan, Manuel Cebrian, Nick Obradovich, Josh Bongard, Jean-François Bonnefon, Cynthia Breazeal, Jacob W Crandall, Nicholas A Christakis, Iain D Couzin, Matthew O Jackson, et al. 2019. Machine behaviour. *Nature* 568, 7753 (2019), 477–486.
- [57] E. M. Rogers. 2003. Diffusion of Innovations (5th ed.). Simon and Schuster.
- [58] Hugo Touvron, Louis Martin, Kevin Stone, Peter Albert, Amjad Almahairi, Yasmine Babaei, Nikolay Bashlykov, Soumya Batra, Prajjwal Bhargava, Shruti Bhosale, Dan Bikel, Lukas Blecher, Cristian Canton Ferrer, Moya Chen, Guillem Cucurull, David Esiobu, Jude Fernandes, Jeremy Fu, Wenyin Fu, Brian Fuller, Cynthia Gao, Vedanuj Goswami, Naman Goyal, Anthony Hartshorn, Saghar Hosseini, Rui Hou, Hakan Inan, Marcin Kardas, Viktor Kerkez, Madian Khabsa, Isabel Kloumann, Artem Korenev, Punit Singh Koura, Marie-Anne Lachaux, Thibaut Lavril, Jenya Lee, Diana Liskovich, Yinghai Lu, Yuning Mao, Xavier Martinet, Todor Mihaylov, Pushkar Mishra, Igor Molybog, Yixin Nie, Andrew Poulton, Jeremy Reizenstein, Rashi Rungta, Kalyan Saladi, Alan Schelten, Silva Ruan, Smith Eric Michael, Subramanian Ranjan, Tan Xiaoqing Ellen, Tang Binh, Taylor Ross, Williams Adina, Xiang Jian, Xu Kuan Puxin, Yan Zheng, Zarov Iliyan, Zhang Yuchen, Fan Angela, Kambadur Melanie, Narang Sharan, Rodriguez Aurelien, Stojnic Robert, Edunov Sergey, and Scialom Thomas. 2023. Llama 2: Open Foundation and Fine-Tuned Chat Models. arXiv preprint arXiv:2310.12345 (2023).
- [59] Amanda L Traud, Peter J Mucha, and Mason A Porter. 2012. Social structure of facebook networks. *Physica A: Statistical Mechanics and its Applications* 391, 16 (2012), 4165–4180.
- [60] Jeffrey Travers and Stanley Milgram. 1977. An experimental study of the small world problem. In *Social networks*. Elsevier, 179–197.
- [61] Veniamin Veselovsky, Manoel Horta Ribeiro, and Robert West. 2023. Artificial Artificial Artificial Intelligence: Crowd Workers Widely Use Large Language Models for Text Production Tasks. arXiv:2306.07899 [cs.CL]

- [62] Jesse Vig, Sebastian Gehrmann, Yonatan Belinkov, Sharon Qian, Daniel Nevo, Yaron Singer, and Stuart Shieber. 2020. Investigating gender bias in language models using causal mediation analysis. Advances in neural information processing systems 33 (2020), 12388–12401.
- [63] Duncan J Watts and Steven H Strogatz. 1998. Collective dynamics of 'small-world' networks. nature 393, 6684 (1998), 440–442.
- [64] Xuhui Zhou, Hao Zhu, Leena Mathur, Ruohong Zhang, Haofei Yu, Zhengyang Qi, Louis-Philippe Morency, Yonatan Bisk, Daniel Fried, Graham Neubig, et al. 2023. Sotopia: Interactive evaluation for social intelligence in language agents. arXiv preprint arXiv:2310.11667 (2023).

# A FULL REGRESSION TABLES

Temp.	$\hat{ heta}_{ ext{PA}}$	$\hat{ heta}_{ m H}$	$\hat{ heta}_{ ext{TC}}$	Log Likelihood	AIC
0.5	0.50*** (0.04)			-2,236.36	4,476.71
0.5		2.78*** (0.07)		-1,511.42	3,026.85
0.5			1.53*** (0.04)	-1,506.01	3,016.02
0.5	0.64*** (0.06)	2.99*** (0.19)		-1,414.71	2,835.41
0.5	-0.02 (0.10)		1.53*** (0.08)	-1,505.95	3,017.90
0.5		1.43*** (0.11)	0.82*** (0.06)	-1,406.39	2,818.78
0.5	0.41*** (0.31)	1.95*** (0.64)	0.59*** (0.37)	-1,377.47	2,762.94
1.0	0.48*** (0.04)			-2,242.85	4,489.70
1.0		2.69*** (0.07)		-1,558.67	3,121.34
1.0			1.47*** (0.04)	-1,556.68	3,117.37
1.0	0.58*** (0.05)	2.86*** (0.08)		-1,473.13	2,952.26
1.0	-0.04 (0.06)		1.47*** (0.06)	-1,556.24	3,118.48
1.0		1.40*** (0.28)	0.79*** (0.06)	-1,457.76	2,921.52
1.0	0.36*** (0.13)	1.85*** (0.52)	0.58*** (0.33)	-1,435.07	2,878.13
1.5	0.50*** (0.04)			-2,233.25	4,470.50
1.5		2.51*** (0.07)		-1,646.83	3,297.65
1.5			1.36*** (0.04)	-1,636.20	3,276.40
1.5	0.57*** (0.07)	2.65*** (0.13)		-1,559.57	3,125.15
1.5	-0.01 (0.05)		1.37*** (0.04)	-1,636.19	3,278.37
1.5		1.29*** (0.11)	0.75*** (0.06)	-1,546.78	3,099.55
1.5	0.36*** (0.16)	1.72*** (0.31)	0.55*** (0.20)	-1,522.47	3,052.94
Note			* : P < 0.05, **	: P < 0.01, *** :	P < 0.001

Table 2. Multinomial logit coefficients for Caltech36. The standard errors of the estimates are shown in parentheses.

Temp.	$\hat{ heta}_{ ext{PA}}$	$\hat{ heta}_{ m H}$	$\hat{ heta}_{ ext{TC}}$	Log Likelihood	AIC
0.5	0.33*** (0.03)			-4,978.28	9,960.56
0.5		2.91*** (0.05)		-3,027.03	6,058.06
0.5			1.37*** (0.02)	-3,014.28	6,032.57
0.5	0.44*** (0.15)	2.99*** (0.10)		-2,948.91	5,903.82
0.5	-0.18*** (0.09)		1.36*** (0.07)	-3,002.17	6,010.35
0.5		1.42*** (0.11)	0.72*** (0.07)	-2,847.16	5,700.32
0.5	0.18*** (0.13)	1.62*** (0.23)	0.65*** (0.08)	-2,838.33	5,684.66
1.0	0.38*** (0.03)			-4,959.02	9,922.04
1.0		2.83*** (0.05)		-3,119.06	6,242.11
1.0			1.32*** (0.02)	-3,118.13	6,240.26
1.0	0.50*** (0.16)	2.92*** (0.09)		-3,018.85	6,043.71
1.0	-0.11** (0.09)		1.32*** (0.07)	-3,113.21	6,232.43
1.0		1.41*** (0.15)	0.69*** (0.11)	-2,947.89	5,901.78
1.0	0.26*** (0.07)	1.70*** (0.35)	0.58*** (0.12)	-2,927.99	5,863.97
1.5	0.36*** (0.03)			-4,952.51	9,909.02
1.5		2.64*** (0.05)		-3,324.71	6,653.43
1.5			1.24*** (0.02)	-3,306.06	6,616.11
1.5	0.44*** (0.11)	2.71*** (0.05)		-3,241.67	6,489.35
1.5	-0.14*** (0.10)		1.24*** (0.05)	-3,298.07	6,602.13
1.5		1.30*** (0.14)	0.67*** (0.09)	-3,150.29	6,306.57
1.5	0.19*** (0.14)	1.50*** (0.33)	0.59*** (0.10)	-3,139.42	6,286.83
Note			* : <i>P</i> < 0.05, **	P < 0.01, *** : I	P < 0.001

Table 3. Multinomial logit coefficients for Swarthmore42. The standard errors of the estimates are shown in parentheses.

Temp.	$\hat{ heta}_{ ext{PA}}$	$\hat{ heta}_{ ext{H}}$	$\hat{ heta}_{ ext{TC}}$	Log Likelihood	AIC
0.5	0.28*** (0.02)			-5,983.56	11,971.13
0.5		2.93*** (0.05)		-3,637.18	7,278.37
0.5			1.11*** (0.02)	-3,740.78	7,485.55
0.5	0.38*** (0.04)	3.06*** (0.21)		-3,523.06	7,052.12
0.5	-0.04 (0.08)		1.11*** (0.04)	-3,739.31	7,484.61
0.5		1.68*** (0.13)	0.51*** (0.07)	-3,477.37	6,960.75
0.5	0.23*** (0.06)	2.00*** (0.24)	0.41*** (0.09)	-3,444.33	6,896.67
1.0	0.28*** (0.02)			-5,982.66	11,969.32
1.0		2.85*** (0.05)		-3,759.78	7,523.56
1.0			1.07*** (0.02)	-3,879.04	7,762.08
1.0	0.36*** (0.07)	2.96*** (0.31)		-3,649.84	7,305.68
1.0	-0.04 (0.06)		1.07*** (0.03)	-3,877.83	7,761.66
1.0		1.67*** (0.11)	0.49*** (0.08)	-3,611.48	7,228.95
1.0	0.23*** (0.10)	1.98*** (0.17)	0.38*** (0.06)	-3,578.18	7,164.36
1.5	0.30*** (0.03)			-3,241.67	6,487.34
1.5		2.71*** (0.06)		-2,145.02	4,294.03
1.5			1.03*** (0.02)	-2,175.32	4,354.64
1.5	0.37*** (0.08)	2.81*** (0.10)		-2,080.67	4,167.34
1.5	-0.01 (0.04)		1.03*** (0.04)	-2,175.25	4,356.49
1.5		1.50*** (0.10)	0.51*** (0.04)	-2,051.61	4,109.23
1.5	0.22*** (0.12)	1.78*** (0.27)	0.41*** (0.07)	-2,033.49	4,074.98
Note			* : P < 0.05, '	** : P < 0.01, *** :	P < 0.001

Table 4. Multinomial logit coefficients for UChicago 30. The standard errors of the estimates are shown in parentheses.

#### **B** FEATURE REPRESENTATIONS FOR PROMPTS

Below, we give examples of the features used in the prompt presented in Algorithm 1. The features are formatted as a list of JSON objects which are provided to the prompt.

# **B.1** Principle 1: Preferential Attachment

For the structure-based information (Figure 1(a)) we have the following features:

And for the degree-based information (Figure 1(b)) we have the following features:

# **B.2** Principle 2: Triadic Closure

For the structure-based information (Figure 3(a)) we have the following features:

```
"name" : 0,
    "common_neighbors" : [5, 7, 1, 6]
},
```

]

And for the degree-based information (Figure 3(b)) we have the following features:

## **B.3** Principle 3: Homophily

We have the following features:

# **B.4** Principle 5: Small-World

We have the following features:

#### **B.5** Real-World Data

We have the following features:

We note that the initial Facebook100 dataset included gender information as a feature. We chose not to include the gender as one of the features as it has been shown that language models exhibit gender bias [12, 35, 62].